# X-ray Diffraction and $^{13}$C Solid-State NMR Studies of the Dimethylformamide Solvate of Tetra(C-undecyl)calix[4]resorcinarene

**Marek Pietraszkiewicz* and Oksana Pietraszkiewicz**

*Institute of Physical Chemistry, Polish Academy of Sciences, ul. Kasprzaka 44/52, 01-224 Warszawa, Poland*

**Waclaw Kolodziejski***

*Department of Inorganic and Analytical Chemistry, Medical University of Warsaw, ul. Banacha 1, 02-097 Warszawa, Poland*

**Krzysztof Wozniak**

*Department of Chemistry, University of Warsaw, ul. Pasteura 1, 02-093 Warszawa, Poland*

**Neil Feeder, Francesca Benevelli, and Jacek Klinowski***

*Department of Chemistry, University of Cambridge, Lensfield Road, Cambridge CB2 1EW, United Kingdom*

*Received: May 14, 1999*

Lipophilic tetra(C-undecyl)calix[4]resorcinarene obtained from resorcinol and lauryl aldehyde forms solvates with many organic solvents. Particularly good quality crystals are obtained from dimethylformamide. Single-crystal X-ray diffraction (XRD) analysis of the solvate shows that the calix[4]resorcinarene molecules form centrosymmetric dimers held by van der Waals interactions of the C-undecyl aliphatic chains. The dimers are associated into layers with hydroxyl groups at the surfaces. Three types of solvent molecules are embedded in the crystal lattice: disordered isolated molecules located just above the cavities formed by the resorcinol units, clusters of four DMF molecules located between the calixarene layers, and single DMF molecules located inside the layers close to the alkyl chains. The solvent molecules join the layers of calix[4]resorcinarenes by means of various hydrogen bonds. The $^{13}$C CP/MAS spectra are in agreement with the XRD results.

## Introduction

Calix[4]resorcinarenes (Scheme 1) have attracted much attention on account of their unusual complexing properties, conformational flexibility, the great variety of ways in which they can be further derivatized, and their easy availability. The prospect of forming multicomponent species involving calix[4]resorcinarenes makes them of interest for molecular recognition,[1−7] transport across membranes,[8,9] ion channels,[10] self-assembling monolayers at the air−water interface[4,11−13] and on metals.[14−18] A fine review of the chemistry of calix[4]resorcinarenes has appeared.[19]

We are interested in calix[4]resorcinarenes as molecular devices for molecular recognition studies in solution by means of HPLC experiments, transport across liquid and supported plastic membranes, in thermochemistry, and NMR. Calixarenes generally form very stable solvates with practically all solvents from which they crystallize. A remarkable number of their solvates is very stable, which may have a considerable impact on molecular recognition phenomena in solution, since the solvent will compete with the species involved in such recognition. It is therefore of interest to study the structure and thermal stability of a range of calixarene solvates, which will lead to a rational choice of solvents suitable for the study of molecular recognition. In this report we use XRD and NMR to examine the molecular and crystal structure of the tetra(C-undecyl)calix[4]resorcinarene (CAV11) (Figure 1) cocrystallized with dimethylformamide.

**SCHEME 1**

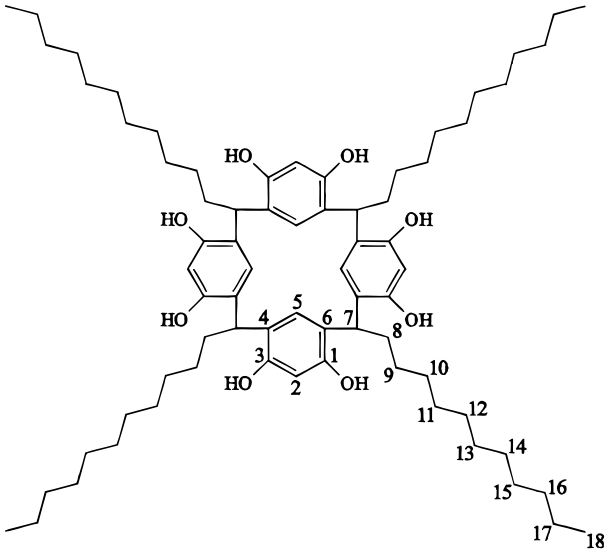


## Experimental Section

**Chemicals.** All reagents were purchased from Aldrich or Merck. The tetra(C-undecyl)calix[4]-resorcinarene complex with dimethylformamide (CAV11/DMF) was prepared as described in the literature.[1] Dimethylformamide (DMF) was distilled under reduced pressure over calcium hydride. CAV11 was crystallized

10.1021/jp991589v CCC: $19.00 © 2000 American Chemical Society
Published on Web 02/09/2000

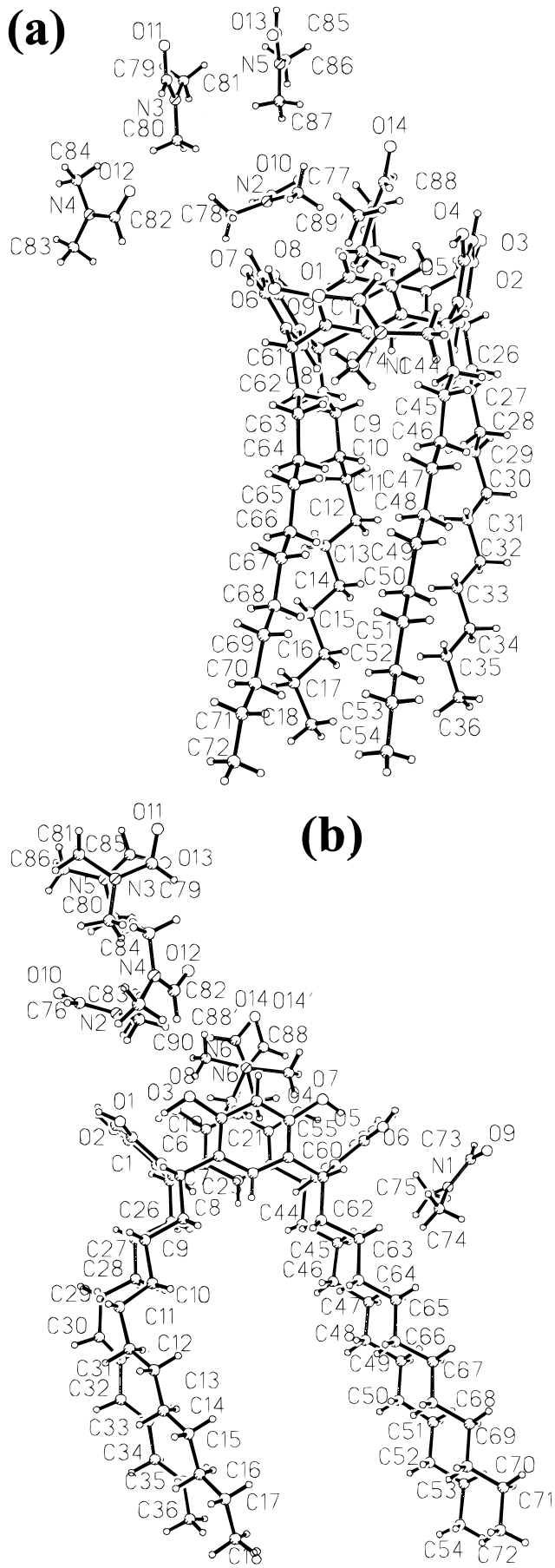


**Figure 1.** Labeling of atoms and a PLUTO drawing of the main part of the complex of CAV11. (a) projection showing the straight aliphatic chains, (b) projection showing the bent aliphatic chains.

**TABLE 1: Crystal Data and Structure Refinement Details for CAV11/DMF**

| | |
|---|---|
| empirical formula | $C_{72}H_{112}O_8 \cdot 6C_3H_7NO$ |
| formula weight | 1550.24 |
| temperature [K] | 293(2) |
| wavelength [Å] | 0.71069 |
| crystal system | triclinic |
| space group | $P\bar{1}$ |
| unit cell dimensions | $a = 13.080(2)$ Å, $\alpha = 99.73(2)^o$ |
| | $b = 30.390(8)$ Å, $\beta = 90.30(1)^o$ |
| | $c = 11.827(2)$ Å, $\gamma = 93.85(2)^o$ |
| volume [Å$^3$] | 4623(2) |
| $Z$ | 2 |
| density (calculated) [mg/m$^3$] | 1.339 |
| absorption coefficient [mm$^{-1}$] | 0.798 |
| $F$(000) | 1708 |
| crystal size [mm$^3$] | 0.20 × 0.30 × 0.25 |
| $\theta$ range for data collection [deg] | 2.52 to 22.53° |
| index ranges | $0 \le h \le 14$, $-32 \le k \le 32$, $-12 \le l \le 12$ |
| reflections collected | 12059 |
| independent reflections | 12059 [R(int) = 0.10] |
| refinement method | full-matrix least-squares on $F^2$ |
| data/restraints/parameters | 12006/0/1036 |
| goodness-of-fit on $F^2$ | 1.053 |
| final $R$ indices [$I > 2\sigma(I)$] | R1 = 0.108, $w$R2 = 0.163 |
| $R$ indices (all data) | R1 = 0.311, $w$R2 = 0.271 |
| extinction coefficient | 0.0019(4) |
| largest difference peak and hole [e·Å$^3$] | 0.34 and −0.31 |

from hot DMF and left for slow cooling. Suitable cubic crystals were obtained after standing for 1 day.

**X-ray Diffraction.** X-ray measurements were made on a Rigaku AFC7R diffractometer using monochromated Mo Kα radiation in the $\omega - 2\theta$ scan mode. Three standard reflections were monitored for every 100 reflections collected, and none showed a significant decrease in standard intensity over the data collection time. The data were corrected for Lorentz and polarization effects. The structure was solved by direct methods[20] and refined using SHELXL-93.[21] The refinement was based on $F^2$ for all reflections, except for those with very negative $F^2$. Weighted $R$ factors $\omega R$, and all goodnesses-of-fit $S$ values, are based on $F^2$. Conventional $R$ factors are based on $F$, with $F$ set to zero for negative $F^2$. The criterion $F^2 > 2\sigma(F^2)$ was used only for calculating $R$ factors and is not relevant to the choice of reflections for the refinement. $R$ factors based on $F^2$ are about twice as large as those based on $F$, and $R$ factors based on all data are even larger. The positions of most hydrogen atoms were calculated geometrically, then fixed and not refined. Scattering factors and absorption coefficients were taken from Tables 6.1.1.4 and 4.2.4.2 of ref 22. Experimental details concerning the collection and refinement of data are listed in Table 1.

**Solid-State NMR.** Solid-state $^{13}$C MAS NMR spectra were recorded at 298 K on a Varian UNITY PLUS-200 spectrometer at 50.3 MHz, using a Doty double-bearing probehead with 7 mm zirconia rotors driven by dry air at 4.3 kHz. The conventional single contact $^1$H → $^{13}$C cross-polarization (CP)[23,24] with reversal of spin temperature in the rotating frame was performed with the 5 s recycle delay (optimized), $\pi/2$ pulses of 6.7 $\mu$s duration, and high-power proton decoupling during signal acquisition. The contact time was varied up to 4.5 ms. The magic angle was set precisely by observing the $^{79}$Br resonance from KBr. The $^{13}$C dipolar-dephased spectra[25] were recorded, to reveal resonances corresponding to weak $^1$H − $^{13}$C dipolar couplings, i.e., to quaternary carbon and methyl peaks, with a 50 $\mu$s time period without proton decoupling prior to acquisition. The liquid-state spectra were measured in $CDCl_3$ on a Varian

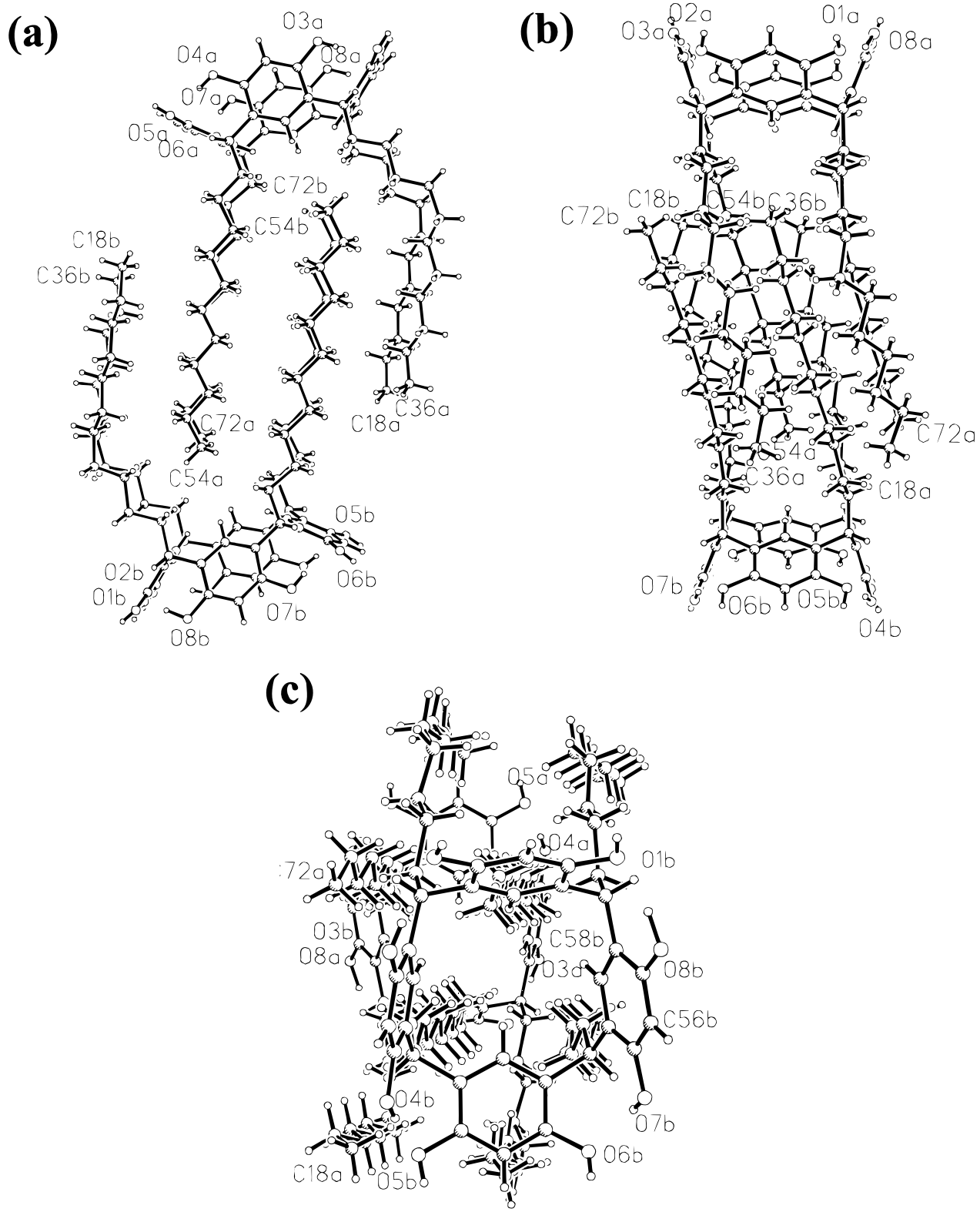


**Figure 2.** Three projections of the molecular dimers: (a) perpendicular to the aliphatic bent carbon chains, (b) perpendicular to the straight aliphatic chains, (c) along the aliphatic chains.

UNITY PLUS-500 spectrometer and the $^{13}$C assignments, based on chemical shifts,[26] were confirmed using DEPT experiments.

## Results and Discussion

**X-ray Data.** The CAV11/DMF complex crystallizes in an asymmetric manner in the triclinic space group $P\bar{1}$ with two molecules in the unit cell (Table 1). The unit cell parameters are $a = 13.080(2)$ Å, $b = 30.390(8)$ Å, $c = 11.827(2)$ Å, $\alpha = 99.73(2)°$, $\beta = 90.30(1)°$, and $\gamma = 93.85°$. The labeling of atoms and two projections of the complex are given in Figure 1. The positional parameters are shown in Table 1 of Supporting Information, which also contain the bond lengths and angles, and numerical values of atomic displacement parameters in Tables 3 and 4.

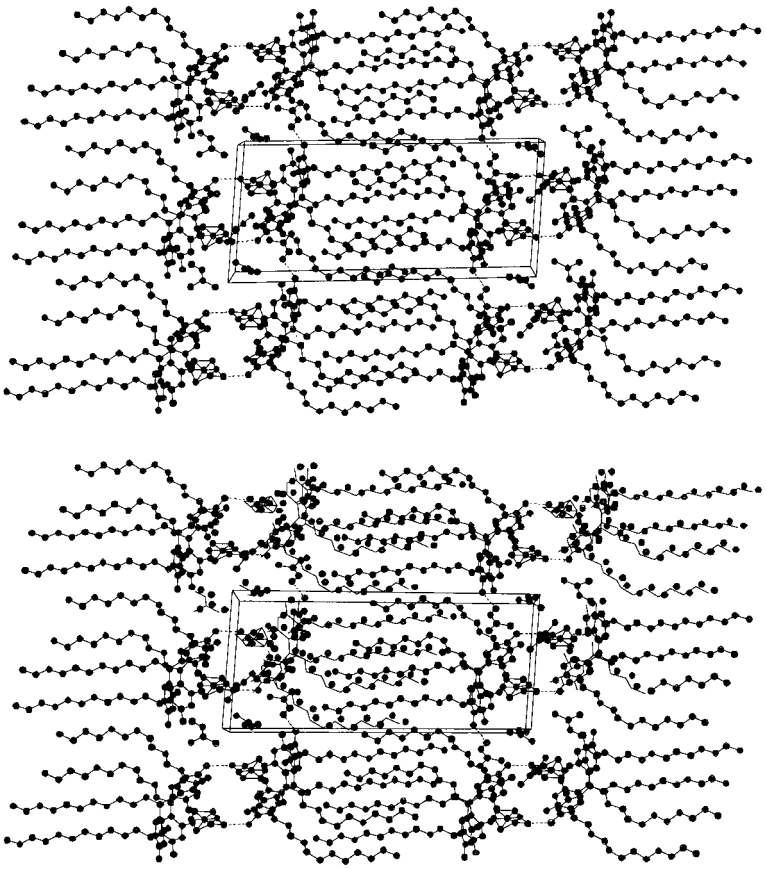

**Figure 3.** Three-dimensional packing of molecules in the crystal lattice with hydrogen atoms omitted for clarity.

CAV11, the main component of the complex, has four long ($C_{11}$) aliphatic chains. Two of them are relatively straight and parallel to each other, while the other two are bent at the fourth carbon atom in the chain starting from the calix[4]resorcinarene part, thus increasing the space between the chains. The far ends of the two bent aliphatic chains are approximately parallel to the straight chains. The space between the aliphatic chains accommodates the straight aliphatic chains of the neighboring molecule related by the center of symmetry (Figure 2), to form molecular dimers in the crystal lattice, which are held together by van der Waals interactions.

The interactions are so strong that the molecular dimers form layers of calixarene molecules with their nonpolar parts inside the layers and the strongly polar parts (hydroxyl groups) at the surface (Figure 3). The layers of calix[4]resorcinarene are held together to form a 3D structure via hydrogen bonds and electrostatic interactions with the solvent molecules.

The polar parts of tetra(C-undecyl)calix[4]resorcinarene are exposed and interact with solvent molecules. There are three types of solvent molecules: single DMF molecules present in the structure just above the cavities formed by resorcinol units, clusters of four DMF molecules in the space between the polar surfaces of the CAV11 layers, and single DMF molecules inside the layers in close proximity to the alkyl chains. Some of the DMF molecules are disordered. In fact, the presence of clusters of solvent molecules between layers covered with hydroxyl groups (Figure 3) closely resembles the situation in inorganic pilared clays.

The aromatic rings of the resorcinarene fragment have their −OH groups in close proximity, thus allowing hydrogen bonding between these groups necessary for forming the calix. The geometry of such close contacts is given in Table 2 of Supporting Information.

**TABLE 2: $^{13}$C NMR Chemical Shifts of the CAV11/DMF Complex in the Solid State and Dissolved in $CDCl_3$**

| carbon atom | solid state | solution |
|---|---|---|
| | Calixarene | |
| C1, C3 | 153.7, 153.1, 151.5, 150.8[a] | 151.4 |
| C2 | 103.4, 102.9, 100.9[b] | 103.2 |
| C4, C6 | 123.2, 122.7, 122.3, 121.2 | 124.5 |
| C5 | 123.7,[c] 120.0[c] | 123.5 |
| C7 | 33.6 | 33.4 |
| C8−C16 | 32.4[d] | 32.0−28.2 |
| C17 | 24.1, 23.4 | 22.7 |
| C18 | 16.5, 15.1, 13.9 | 14.1 |
| | DMF | |
| C−H | 163.2 | 162.8 |
| methyl groups | 35.5, 30.4 | 36.2, 31.4 |

[a] Shoulder. [b] Approximately the same intensity as for the (103.4 + 102.9) joint peak. [c] Probably an overlapped doublet, see Figure 3. [d] At the top of a large, wide and complex peak.

**Solid-State NMR.** The solid-state spectrum of CAV11/DMF was assigned by reference to the solution spectrum in $CDCl_3$, and on the basis of dipolar dephasing and variable-contact time experiments (Table 2). The NMR peaks are denoted according to Scheme 1. The spectrum is very well resolved in the calix region (Figures 4−6). In principle, peak multiplicity should be equal to the number of chemically equivalent carbon atoms in the calixarene moiety, because they are crystallographically inequivalent. Thus, assuming sufficient spectral resolution, we should detect eight components for the (C1 + C3) and (C4 + C6) peaks, and four components for the C2 and C5 peaks.

We note that there are two kinds of hydroxyl groups at the calix, depending on their role in the hydrogen bonding. Thus the oxygen atoms O(8), O(3), O(4), and O(7) donate protons to the hydroxyl oxygen atoms O(1), O(2), O(5), and O(6),

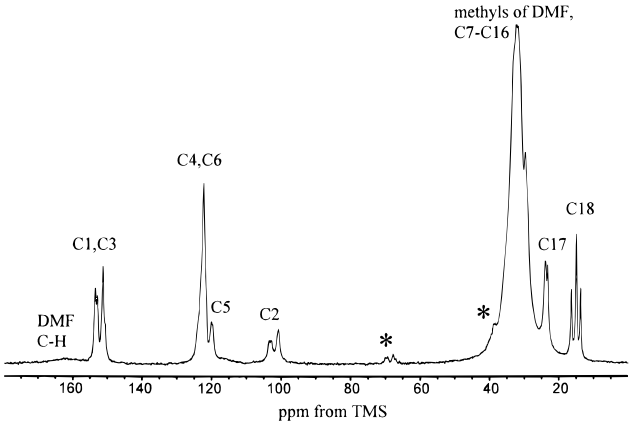


**Figure 4.** $^{13}$C CP/MAS NMR spectrum of the CAV11/DMF crystals, recorded with 4 ms contact time. Asterisks denote spinning sidebands.

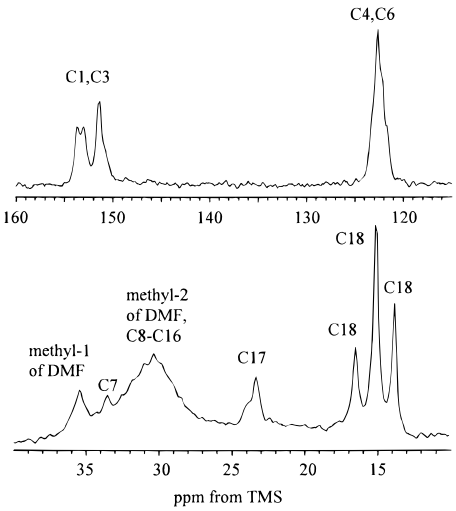


**Figure 5.** Dipolar-dephased $^{13}$C CP/MAS NMR spectrum of the CAV11/DMF crystals. Peaks C2 and C5 are absent from the spectrum, while the C7 and $CH_2$ peaks are still visible, probably due to segmental mobility of the aliphatic chains.

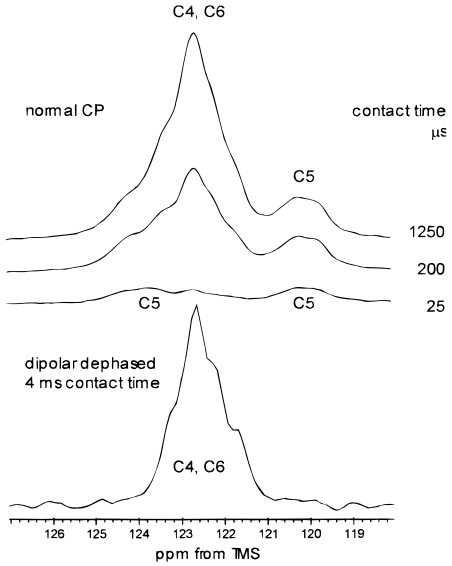


**Figure 6.** Normal CP (upper three plots) and dipolar-dephased (bottom) $^{13}$C spectra of C5, C4 and C6 peaks. The normal CP spectra are shown for various contact times on the same intensity scale.

respectively, forming intramolecular hydrogen bonds (Figure 1b). At the same time, the O(1), O(2), O(5), and O(6) oxygens are involved as proton donors in intermolecular hydrogen

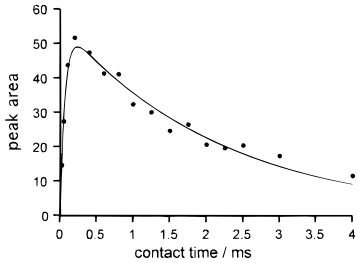


**Figure 7.** Dependence of the intensity on the contact time for the C−H peak of DMF at 163.2 ppm.

bonding. This means that there are two types of aromatic rings (Figure 1b). The first kind is the ring with O(8) and O(3) and the ring with (O4) and (O7). The second kind is the ring with O(1) and O(2) and the ring with O(5) and O(6). Indeed, C2 (Figure 4) and C5 (Figure 6) give doublets, the components of which show further minor splittings. Then, C4 and C6 give together four peaks (Figures 5 and 6), while doublets from C1 and C3 are strongly overlapped (Figures 4 and 5). It follows that the splittings of the calix peaks are related to the hydrogen bonding.

The peaks from the aliphatic chains overlap substantially (Figures 4 and 5), which prohibits their detailed analysis. The only obvious feature is that two methyl groups have the same chemical shift, thus giving a 1:2:1 "false triplet". The solid-state chemical shifts are close to those in the $CDCl_3$ solution (Table 2).

The CP kinetics of calixarene nuclei require detailed discussion and the consideration of various kinetic models, and will be discussed elsewhere. Here, we are concerned with the structure of the calixarene/DMF crystals, so that the cross-polarization behavior of DMF is of great importance. The intensity of the C−H peak of DMF is a typical double-exponential function of the contact time[24] (Figure 7). One observes an initial increase with a $T_{CP}$ time constant of $65 \pm 7$ $\mu$s, a maximum for the optimum contact time of 0.23 ms, and a final decay with a time constant of $2.2 \pm 0.2$ ms, which is a proton spin−lattice relaxation time in the rotating frame. One observes an initial increase with a $T_{CP}$ time constant of $65 \pm 7$ $\mu$s, a maximum for the optimum contact time of 0.23 ms and a final decay with a time constant of $2.2 \pm 0.2$ ms, which is the proton spin−lattice relaxation time in the rotating frame. The values for the rotating-frame spin−lattice relaxation time of protons in calixarene are very different from that of DMF and vary in the 6−10 ms range, increasing from the aromatic ring, through the aliphatic chain to the tail methyl groups. It is therefore clear that the DMF carbons cross-polarize from the DMF protons, not from the remote protons of calixarene. This agrees very well with the XRD results, which locate the DMF molecules outside the calices and between the calixarene molecules.

Van Wageningen et al.[27] measured solid-state $^{13}$C CP/MAS and $^{2}$H NMR spectra of a calixarene-based carcerand, claimed to be complexed with DMA or DMSO. The carcerand contained the resorcinarene moiety similar to that described here. Unfortunately, the $^{13}$C spectra are poorly resolved and do not prove that complexation has occurred. The only conclusion, the cavity walls of the carcerand are rigid, is based on dipolar dephased spectra recorded with much too long (40 ms instead of 40 $\mu$s) dephasing delay. Also, the delay in the quadrupole echo sequence used for recording the $^{2}$H spectra was much too long. The energy difference calculated from the variable-temperature $^{2}$H spectra was comparable to the molecular transational energy at 298 K. This means that a small DMSO molecule can easily

escape from the cavity, so that the two sites postulated for the molecule can reside inside and outside the cavity. Our work shows that solvent molecules can be located far from the cavity, even in the region of the $C_{11}$ chains. It is clear that the combination of single-crystal X-ray diffraction and solid-state NMR leads to valuable insights into calixarene complexes.

**Acknowledgment.** J.K., W.K., and K.W. are grateful to the British Council and the Polish Committee for Scientific Research for financial support within the Project WAR/992/131. M.P. and O.P. thank the Polish Committee for Scientific Research for Grant 3T09A 025 011.

**Supporting Information Available:** Tables of atomic coordinates and structural parameters for CAV11/DMF. This material is available free of charge via the Internet at http://pubs.acs.org.

## References and Notes

(1) Aoyama, Y.; Tanaka, Y.; Toi, H.; Ogoshi, H. *J. Am. Chem. Soc.* **1988**, *110*, 634.

(2) Aoyama, Y.; Uzawa, T.; Saita, K.; Tanaka, Y.; Toi, H.; Ogoshi, H. *Tetrahedron Lett.* **1988**, *29*, 5271.

(3) Aoyama, Y.; Tanaka, Y.; Sugahara, S. *J. Am. Chem. Soc.* **1989**, *111*, 5397.

(4) Kurihara, K.; Ohto, K.; Tanaka, Y.; Aoyama, Y.; Kunitake, T. *J. Am. Chem. Soc.* **1991**, *113*, 444.

(5) Schneider, U.; Schneider, H.-J. *Chem. Ber.* **1994**, *127*, 2455.

(6) Leigh, D. A.; Linnane, P.; Pritchard, R. G.; Jackson, G. *J. Chem. Soc., Chem. Commun.* **1994**, 389.

(7) Schneider, H.-J.; Schneider, U. *J. Inclusion Phenom., Mol. Recognit. Chem.* **1994**, *19*, 67.

(8) Koide, Y.; Sato, H.; Shosenji, H.; Yamada, K. *Bull. Chem. Soc. Jpn.* **1996**, *69*, 315.

(9) Jin, T.; Kinjo, M.; Koyama, T.; Kobayashi, Y.; Hirata, H. *Langmuir* **1996**, *12*, 2684.

(10) Tanaka, Y.; Kobuke, Y.; Sokabe, M. *Angew. Chem., Int. Ed. Engl.* **1995**, *34*, 693.

(11) Moreira, W. C.; Dutton, P. J.; Aroca, R. *Langmuir* **1994**, *10*, 4148.

(12) Davis, F.; Stirling, C. J. M. *Langmuir* **1996**, *12*, 5365.

(13) Moreira, W. C.; Dutton, P. J.; Aroca, R. *Langmuir* **1995**, *11*, 3137.

(14) van Velzen, E. U. T.; Engbersen, J. F. J.; Reinhoudt, D. N. *Synthesis (Stuttgart)* **1995**, 989.

(15) van Velzen, E. U. T.; Engbersen, J. F. J.; Delange, P. J.; Mahy, J. W. G.; Reinhoudt, D. N. *J. Am. Chem. Soc.* **1995**, *117*, 6853.

(16) Huisman, B. H.; Kooyman, R. P. H.; van Veggel, F. C. J. M.; Reinhoudt, D. N. *Adv. Mater.* **1996**, *8*, 561.

(17) Schönherr, H.; Vancso, G. J.; Huisman, B.-H.; van Veggel, F. C. J. M.; Reinhoudt, D. N. *Langmuir* **1997**, *13*, 1567.

(18) Adams, H.; Davis, F.; Stirling, C. J. M. *J. Chem. Soc., Chem. Commun.* **1994**, 2527.

(19) Timmerman, P.; Verboom, W.; Reinhoudt, D. N. *Tetrahedron* **1996**, *52*, 2663.

(20) Sheldrick, G. M. *Acta Crystallogr.* **1990**, *A46*, 467.

(21) Sheldrick, G. M. *SHELX93. Program for the refinement of crystal structures;* University of Göttingen, Germany, 1993.

(22) Wilson, A. J. C., Ed. *International Tables for Crystallography*; Kluwer: Dordrecht, 1992; Vol. 1.

(23) Pines, A.; Gibby, M. G.; Waugh, J. S. *J. Chem. Phys.* **1973**, *59*, 569.

(24) Mehring, M. *High-Resolution NMR Spectroscopy in Solids*, 2nd ed.; Springer-Verlag: New York, 1983.

(25) Opella, S. J.; Frey, M. H. J. *J. Am. Chem. Soc.* **1979**, *101*, 5854.

(26) *ACD/CNMR Program Version 1.1*; Advanced Chemistry Development, Inc.: Toronto, 1995.

(27) van Wageningen, A. M. A.; Verboom, W.; Zhu, X.; Ripmeester, J. A.; Reinhoudt, D. N. *Supramol. Chem.* **1998**, *9*, 31.